brief communication

A polymorphism peculiar to bipolar actin bundles

Noreen R. Francis and David J. DeRosier
Rosenstiel Basic Medical Sciences Research Center, Brandeis University, Waltham, Massachusetts 02254 USA

ABSTRACT Both muscle and nonmuscle actins produced magnesium paracrystals which we found indistinguishable from one another. Contrary to some previous reports, calcium ions caused no change in filament organization for either type of actin. The most ordered paracrystals consisted of hexagonally packed filaments with opposite polarities. We suggest that this mode of packing permits a form of disorder not previously described, which may account for some puzzling aspects of earlier observations and may prove useful in analyzing actin bundles formed, for example, with erythrocyte band 4.9 protein.

INTRODUCTION

Despite their use in studies of filament structure, we do not know the packing scheme of filaments in actin paracrystals, but we know it is polymorphic. For example, Gillis and O'Brien (1975) and O'Brien et al. (1975) suggested that magnesium paracrystals of thin filaments, (actin with tropomyosin and troponin) exhibited differences in the twist as a consequence of differences in calcium ion concentration. Decoration of their high-calcium paracrystals with S1-fragment of myosin indicated that filaments were present with opposite polarities. Optical diffraction patterns of high-calcium paracrystal images showed intermediate row lines indicating two filaments in the repeating unit, consistent with one filament up and one filament down in the unit cell. These paracrystals had a symmetry of 28 units in 13 turns, distinct from that of magnesium paracrystals of pure actin (13 units in 6 turns). The troponin appeared as a series of transverse bands with a 380-Å repeat. In comparison, the low-calcium paracrystals of thin filaments lacked transverse stripes, had a symmetry of 13 units in 6 turns, and had no intermediate (or half) row lines in their optical transforms. These paracrystals seemed to be identical to magnesium paracrystals of pure actin, and O'Brien and his collaborators concluded that, in these forms, all filaments had the same polarity.

Fowler and Aebi (1982) noted that polylysine-induced paracrystals exhibited a range of polymorphic forms that differed for nonmuscle and muscle actins. Moreover, within one class of polymorphs, paracrystals that looked identical showed differences in their optical transforms, with one set of optical transforms having half row lines and the other lacking half row lines. Unlike paracrystals studied by Gillis and O'Brien, calcium had no effect on the form of the paracrystal or the twist of its component filaments. S1 decoration of dissolving paracrystals showed filaments with opposite polarities in the same bundle, but the relative orientation of adjacent filaments was unclear. Because Fowler and Aebi found no difference in the filament twist in the various polymorphic forms, they suggested that the differences in structure resulted from variations in the axial stagger of filaments, and they accounted for the variety of observed polymorphs and their optical transforms with this staggered packing.

The angle-layered aggregate, a two-sheet structure made from actin filaments, has filaments of opposite orientation in the two sheets (Egelman et al. [1983]). These structures form in the presence of magnesium and often coexist with and merge into paracrystals. Egelman and DeRosier (1983) suggested that these aggregates and paracrystals are related structures which involve a bipolar magnesium bond between filaments. They demonstrated this relationship by simulating images of the paracrystals using the packing scheme derived from the angle-layered aggregates. In this scheme, oppositely oriented filaments had a fixed axial stagger which was the same for both angle-layered aggregates and magnesium paracrystals. They assumed a tetragonal packing of filaments in which adjacent filaments had alternating polarities. There was no evidence to indicate which lattice or lattices existed in paracrystals. In fact, in transverse sections of magnesium paracrystals, Matsudaira et al. (1983) found no regular lattice.

We undertook a study of actin magnesium paracrystals to determine (*a*) if magnesium paracrystals were indeed bipolar, (*b*) if there was an underlying lattice describing filament packing, (*c*) if calcium alters that packing, and (*d*) if nonmuscle and muscle actin produce different paracrystals.

MATERIALS AND METHODS

We purified chicken pectoralis actin according to the method of Spudich and Watt (1971). Dr. Joel Pardee generously supplied the *Dictyostelium discoideum* actin, and Dr. Donald Winkelmann and Dr. Susan Lowey gave us the myosin-S1 fragment. Paracrystals formed upon mixing F-actin with magnesium chloride (20–50 mM) in phosphate buffer (5 mM), pH 7, and 1 mM EDTA (low calcium) or 0.01 mM calcium chloride (high calcium). For microscopy, we put 5 μL of the paracrystal preparation on a carbon-coated grid and stained it with 2% uranyl acetate.

To reveal the polarity of the filaments, we placed magnesium paracrystals (1–5 mg/ml) in low or high calcium on a carbon-coated grid and frayed them in a low-magnesium buffer (5 mM phosphate, 10 mM magnesium chloride, 1 mM EDTA, or 0.01 mM calcium chloride). Incubation of the grids for 30 min at 4°C in fraying buffer containing 25 μg/ml of S1 resulted in frayed bundles with decorated ends. We then rinsed the grids and stained them with 2% uranyl acetate.

To determine the packing of the filaments in the bundles, we examined thin sections of fixed paracrystals. We fixed paracrystals (0.5 mg/ml) in 1.5% tannic acid, 1% glutaraldehyde, 20–50 mM magnesium chloride, and 5 mM phosphate buffer for 15 min at room temperature, spun them at 24,000 *g* for 20 min to form a soft pellet, resuspended the pellet in fixative overnight at 4°C in the dark, washed with cold (0°C) distilled water, postfixed in 1% OsO_4 at 0°C for 30 min, washed in distilled water, en bloc stained in 0.5% uranyl acetate, dehydrated with acetone, embedded in Polybed 812, sectioned with a LKB Huxley ultramicrotome, and stained with lead citrate and uranyl acetate. We examined the grids with a Philips 301 or 420 electron microscope.

RESULTS

Fig. 1 *a–c* shows images of three preparations of paracrystals (chicken pectoralis actin in high calcium and in low calcium and *D. discoideum* actin in high calcium). The images and their computed diffraction patterns (Fig. 1 *d–f*) reveal no differences among the three classes of paracrystals. By measuring the axial positions of the first and sixth layer lines on the diffraction patterns, we determined the number of actin subunits per turn of the helix (DeRosier and Censullo, 1981). In all three types of paracrystals, the repeat of the actin helix was 2.167 ± 0.002 units per turn or 13 units in 6 turns. The variation was due to the accuracy with which layer lines were measured and therefore did not demonstrate any real differences among the paracrystals. We found no variation in the helical symmetry or packing. Thus, the three types of paracrystals appeared indistinguishable. We found no evidence of the axial stagger seen by Fowler and Aebi (1982) for polylysine-induced paracrystals.

We determined the polarity of the paracrystals by decoration of fraying bundles with myosin-S1 fragment. In both high- and low-calcium conditions, the bundles were bipolar as shown in Fig. 2, *a* and *b*. We then examined thin sections of fixed paracrystals (Fig. 3, *a* and *b*) to determine the packing of the filaments in these bundles. Unlike the results of Matsudaira et al. (1983), the transverse sections showed hexagonal packing, with only a modest amount of disorder.

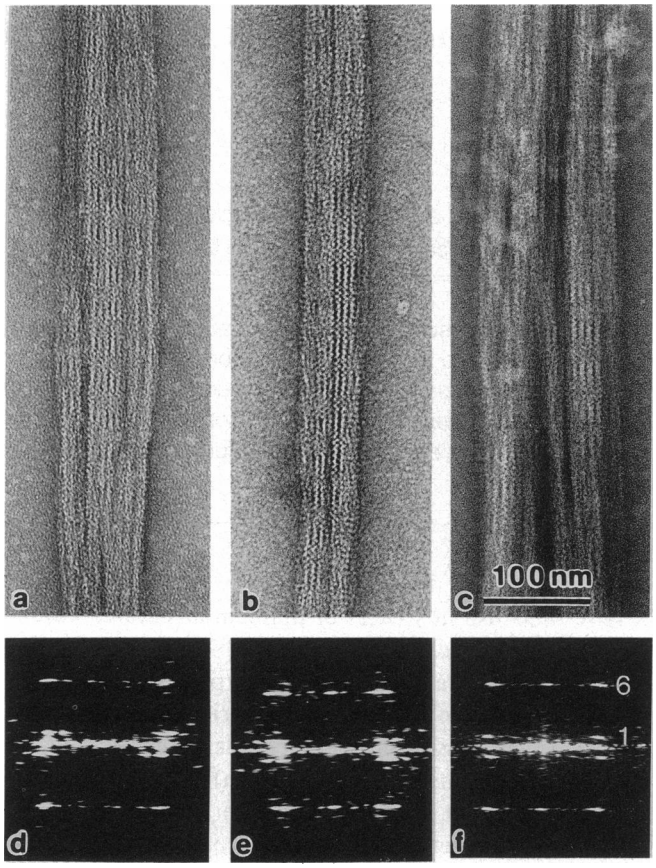

FIGURE 1 Magnesium paracrystals of actin and their transforms. In *a* and *b* the source of actin was chicken skeletal muscle, whereas that in *c* was a nonmuscle source (*D. discoideum*). The paracrystals in *a* and *c* grew in the presence of 0.01 mM calcium chloride, and in *b* in the presence of 1 mM EDTA. Diffraction patterns of the central regions of the images are shown in *d*, *e*, and *f*, respectively. The key features of the patterns are the first and sixth layer lines as indicated in *f*. Note that the strong reflections on these layer lines form vertical rows or row lines. This alignment of reflections arises from the alignment of filaments in the bundle. Note that the diffraction patterns, like the images, reveal no difference among the three kinds of bundles.

DISCUSSION

How do our results compare with those obtained on other types of paracrystals? We suggest that the high-calcium form of thin filament paracrystals seen by Gillis and O'Brien (1975) is quite different from the magnesium paracrystals of plain actin, because in the former the interfilament connections must involve the tropomyosin and/or the troponin directly. There are two reasons for concluding this. First, the symmetry of the filaments is

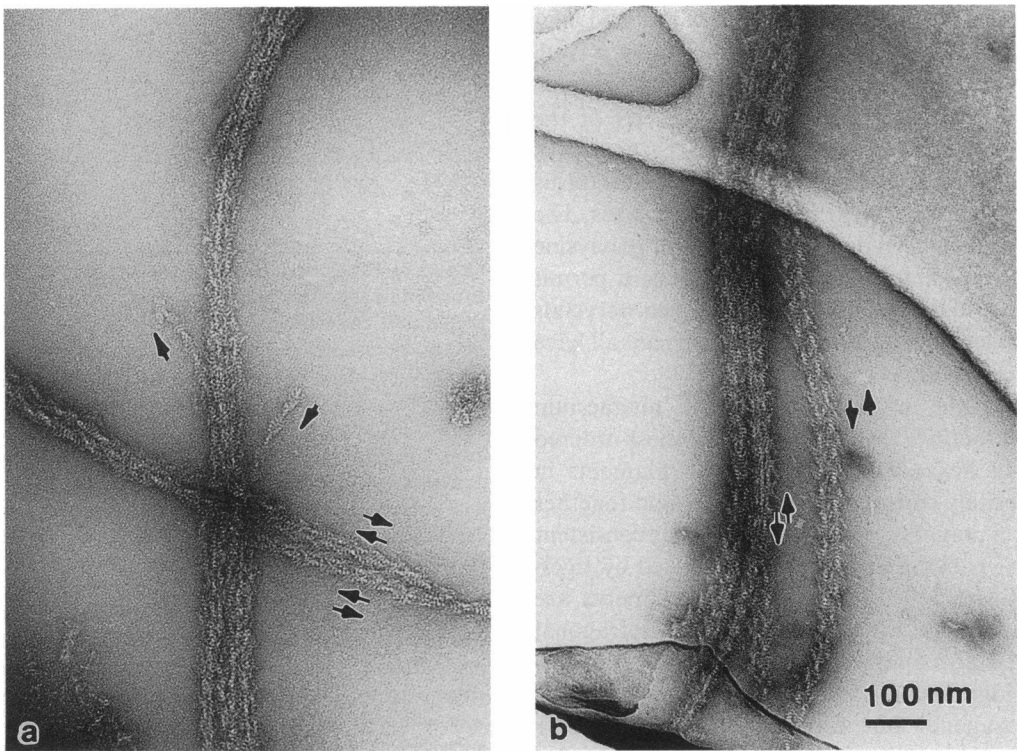

FIGURE 2 Paracrystals of chicken skeletal actin grown decorated with the S1 fragment of myosin. In *a*, the paracrystals are grown in the presence of 0.01 mM calcium chloride, whereas in *b*, paracrystal formation occurred in the presence of 1 mM EDTA. The arrows indicate the polarity of the filaments composing the bundle. Note that filaments of both polarities are present in each bundle.

different from that in other paracrystals and reflects the repeat of the tropomyosin-troponin complex on actin. Second, if the troponin or tropomyosin subunits were not directly involved, the troponin subunits would not align to produce 380-Å transverse bands, but would instead be distributed throughout the 380-Å repeat. The low-calcium form of the thin filament paracrystals, however, appeared identical to the magnesium paracrystals of pure actin, and we suggest both have the same packing.

The polylysine paracrystals, like the magnesium

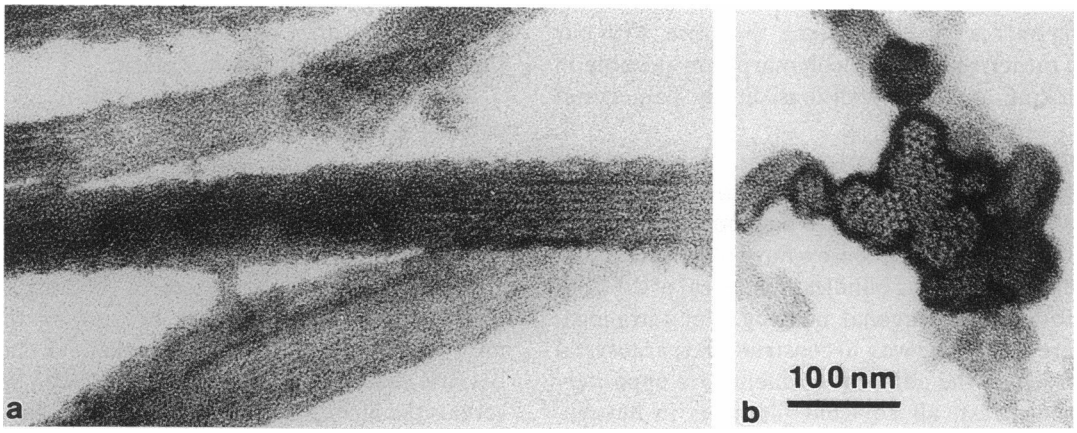

FIGURE 3 Longitudinal (*a*) and transverse (*b*) sections through a paracrystal of chicken skeletal actin grown in the presence of 1 mM EDTA. Note the similarity of the image in *a* with that of the paracrystals in Fig. 1, *a–c*. Note that the filaments seen end on in *b* are arranged on a hexagonal lattice.

paracrystals, appeared to have oppositely oriented filaments linked by bridges of polyvalent cations. With polylysine, however, the most striking polymorphism seemed to arise from variations in axial stagger of the filaments. This was absent in magnesium paracrystals. The types of bridges formed in the two paracrystal forms therefore were not identical, at least not in all cases. The difference could have been due to the length of polylysine molecule relative to magnesium ion which could permit other modes of bridging. Thus, although all paracrystals have actin filaments in both polarities, they do not all have the same bonding rules.

What then is the organization in the magnesium paracrystal of F-actin? The structure in its most ordered form consists of hexagonally packed actin filaments in which the oppositely oriented filaments are held together presumably by a magnesium ion bridge. This is consistent with the bipolar packing arrangement proposed by Egelman and DeRosier (1983), although the filaments are packed in a hexagonal lattice rather than a tetragonal one. Even given strict adherence to a specific, bipolar magnesium bridge between filaments, the bundle lattice needn't be hexagonal but could be disordered. This potential for disorder is illustrated in polar actin bundles such as those found in the inner ear of vertebrates. In some species, bundles have liquid order and, in other species, hexagonal order. DeRosier et al. (1980) showed that because of actin's helical symmetry and angular disorder, actin filaments allow variability in packing while maintaining an ability to make stereospecific bonds with cross-bridging molecules. The degree of order can be changed by varying the conditions under which bundles are assembled (Stokes, D. L. and D. J. DeRosier, unpublished observations). The same considerations apply to bipolar filament packing in which cross-links are only allowed between oppositely oriented filaments. The disordered lattice seen by Matsudaira et al. (1983) in magnesium paracrystals is not inconsistent, therefore, with our results, but rather reflects the polymorphism possible in filament packing and the conditions during paracrystal assembly.

Even with perfect hexagonal packing, however, there needn't be perfect order in a paracrystal. There is the possibility of an interesting form of polymorphism, which is different from that suggested by Fowler and Aebi and which is peculiar to bipolar bundles. This form of disorder is not possible with tetragonal packing. For tetragonal packing, there is only one way to construct the paracrystal (Fig. 4 *c*) in which the adjacent filaments are oppositely oriented. In contrast, all adjacent filaments in hexagonally packed paracrystals cannot be in opposite orientations (Fig. 4, *a* and *b*). As a consequence, there is more than one way to arrange the filaments with the same bonding rule. We found no simple way to enumerate all

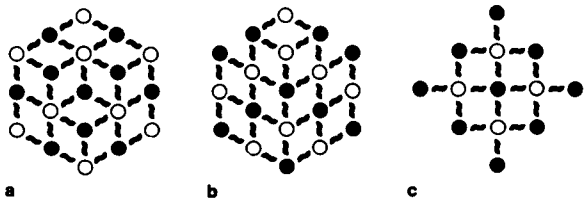

FIGURE 4 Schematic transverse sections of two computer-generated paracrystals showing the polarity of the filaments and the positions of the possible cross-bridges. In *a* and *b*, segments of two of the possible hexagonal packings are shown, whereas in *c*, a segment of the unique tetragonal packing is shown. The patterns were generated by a Monte Carlo program. (*Open circles*) Filaments in the up orientation. (*Solid circles*) Filaments in the down orientation. Tildes indicate the bipolar cross-bridges hypothesized for the paracrystals. The arrangements in *a* and *b* are different because they were generated by different pseudorandom number sequences. The program chooses an up or down orientation depending on the filament's neighbors. If the program were to add a filament to the outside of the bundle in *a*, it could add a filament in either orientation and still make bonds to one of its two neighbors. In the paracrystal in *b*, filaments added at the 2 o'clock and 10 o'clock positions can only be oriented up if bridges to the neighboring filaments must be made. The remainder of the positions could be filled by filaments of either polarity. Unlike the case with hexagonal bundles, there is only one way to form the tetragonal structure shown in *c*. Moreover, any filament added to this bundle must be oriented up in order to bond to the bundle.

different possible arrangements of filaments for a fixed bundle size. To explore the possible arrangements, therefore, we developed a Monte Carlo computer program that generated bundles containing 19 filaments on a hexagonal lattice. Each bundle had the same lattice but the polarities of the filaments varied subject to the condition that in no triangle of three adjacent filaments were all filaments of the same polarity. This ensures that all filaments will be maximally bonded (apart from those at the edge of the bundle). Relaxing this condition increases the number of possible bundles but the additional bundles tend to have fewer cross-bridges. We chose the more restrictive conditions to illustrate the polymorphism.

Using a random number generator to choose filament polarity where either polarity was allowed, we generated a number ($n = 17$) of bundles. Of the 17 packings the program generated, only two were, by chance, identical, suggesting that the number of different possible arrangements is rather large. We selected two packings (Fig. 4, *a* and *b*) from the set of 17 and simulated an electron micrograph of each by viewing the bundle in projection as shown in Fig. 5, *a* and *b*. We chose these two because one image (Fig. 4 *a*), when seen in projection, reveals the bipolar nature of the bundle, whereas the other image (Fig. 4 *b*) masks it. Fig. 5, *c* and *d*, shows the corresponding diffraction patterns. The image in Fig. 5 *a* showed details consistent with an alternation in "filament" polarity in adjacent rows and, as expected, the diffraction

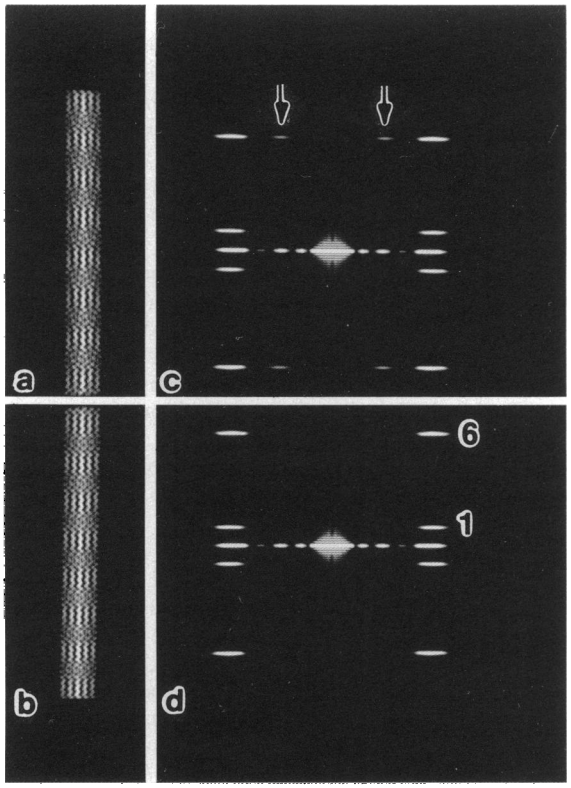

FIGURE 5 Simulated images (*a* and *b*) of bundles having the filament organization shown in Fig. 4, *a* and *b*, respectively. The direction of view is, of course, perpendicular to the long axis of the bundles from 6 to 12 o'clock. The image is a sum of the filaments along the vertical row lines, reflecting the large depth of field in the electron microscope. Thus, the left-hand "filament" in *a* corresponds to the sum of the two up and one down filament in the left-hand vertical row of the image in Fig. 4 *a*. The image of this "filament" is dominated by up filaments. The next "filament" in *a* is dominated by down filaments (three down and one up). The rows in this bundle continue to alternate in this fashion so that the "filaments" in *a* alternate in apparent polarity. In *b*, there is no such alternation of apparent polarity because the filaments do not by chance alternately predominate in the up and then the down polarity. The alternating polarity can be seen as chevrons in *a* by tilting the image and viewing it at a shallow angle along the filament axis. The image in *b* does not show this pattern of chevrons. The bundle in Fig. 4 *b* if projected along the 4 o'clock rather than the 6 o'clock direction, would show an alternation in polarity. Thus, the appearance of alternating polarity in the image depends not only on the packing but on the direction of view. Diffraction patterns of the images in *a* and *b* are shown in *c* and *d*, respectively. The first and sixth layer lines are marked in *d*. Note that there are also row lines arising from the alignment of filaments but that in *c*, there are additional "half" row lines (*arrowheads*) which are absent in *d*. These arise from the apparent alternation in "filament" polarity in *a*.

pattern (Fig. 5 *c*) displayed the half row lines. The image in Fig. 5 *b*, however, revealed a bundle that lacked the alternation of "filament" polarity. We put the word filament in quotation marks because what we see as a "filament" in the image is really a superposition of filaments at different depths in the bundle (i.e., each "filament" in the image in Fig. 5, *a* and *b*, is an average of all the filaments within one vertical row in Fig. 4, *a* and *b*). If the filaments in a row were equally distributed half up and half down, then the averaged "filament" seen in the image lacked polarity. If the filaments pointing up outnumbered those of opposite polarity, then the "filament" in the image possessed up polarity. The "filaments" in Fig. 5 *a* revealed an alternating pattern of up and down polarity because, by chance, the filaments averaged in each row were not equally distributed in their polarities and because, again by chance, adjacent rows favored filaments of opposite polarities. Remember that there is no intrinsic difference of packing in the two bundles in Fig. 4, *a* and *b*, and indeed the same bundle can display these differences when viewed from two different directions (see the caption to Fig. 5). Thus, given this kind of disorder in bundles, some images will exhibit the alternating polarity of filaments and some will not, depending on the particular arrangement of filaments and the particular direction of view (or projection). Correspondingly, some diffraction patterns will show half row lines and some not. Thus, the variability in the packing explains the variability observed by Fowler and Aebi in which the transforms of some paracrystals had half row lines and some did not. In fact, the simplest explanation of their observations is that all the bundles were in fact bipolar.

Hexagonal, disordered bundles have an entropic advantage over perfectly ordered, tetragonal bundles as a consequence of the disorder. A filament must have the correct polarity before it can add to an (ordered) tetragonal bundle at some particular lattice position. Thus, any filament added to the bundle in Fig. 4 *c* must point up (corresponding to an open circle in the figure). To add a filament to a disordered, hexagonal bundle, a filament can often have either polarity. Thus, a filament of either polarity can be added to any position in the hexagonal bundle in Fig. 4 *a*. If the filament can be added in either orientation, the rate of addition of filaments and the equilibrium constant for bundle formation will be doubled over that for the tetragonal bundle.

We propose the disordered, hexagonal packing as a model for the magnesium paracrystal. There is circumstantial evidence supporting the model, and it explains puzzling observations such as those of Fowler and Aebi regarding the half row lines. We cannot yet prove the model because, unfortunately, we have not found a way to determine directly the polarity of each filament in a bundle.

Although the model is based on magnesium paracrystals which do not occur in vivo, it may have direct relevance to understanding the organization of filaments in other types of actin bundles. Bundles such as those made from actin and villin in vitro (Matsudaira and

Burgess, 1982; and DeRosier, D. J., unpublished observations) do not conform to the rules derived from well-understood polar bundles, such as actin-fascin bundles (DeRosier et al., 1977); that is, they lack the transverse bands characteristic of a regular lattice of polar filaments held by specific cross-bridges between adjacent filaments. Another type of bundle which lacks transverse bands is the bundle made from the erythrocyte band 4.9 protein and actin. This type of bundle appears to be bipolar (Owen, C., A. Husain, D. J. DeRosier, and D. Branton, unpublished observations). The filament organization and its polymorphism we propose may be a model for filament organization in these systems.

We thank Judith Black for her excellent photographic work.

This research was supported by a grant from the National Institutes of Health (NIH), GM26357, and a shared instrumentation grant also from the NIH, RR04671.

Received for publication 16 March 1990.

REFERENCES

DeRosier, D. J., and R. Censullo. 1981. Structure of F-actin needles from extracts of sea urchin oocytes. *J. Mol. Biol.* 146:77–99.

DeRosier, D., E. Mandelkow, A. Silliman, L. Tilney, and R. Kane. 1977. Structure of actin-containing filaments from two types of non-muscle cells. *J. Mol. Biol.* 113:679–695.

DeRosier, D. J., L. G. Tilney, and E. H. Egelman. 1980. Actin in the inner ear: the remarkable structure of the stereocilium. *Nature (Lond.).* 287:291–296.

Egelman, E. H., N. Francis, and D. J. DeRosier. 1983. Helical disorder and filament structure of F-actin are elucidated by the angle-layered aggregate. *J. Mol. Biol.* 166:605–629.

Egelman, E. H., and D. J. DeRosier. 1983. Structural studies of F-actin. *In* Actin: Structure and Function in Muscle and Non-Muscle Cells. C. G. dos Remedios and J. A. Barden, editors. Academic Press, Inc., New York. 17–24.

Fowler, W. H., and U. Aebi. 1982. A consistent picture of the actin filament related to the orientation of the actin molecule. *J. Cell Biol.* 93:452–458.

Gillis, J. M., and E. J. O'Brien. 1975. The effect of calcium ions on the structure of reconstituted muscle thin filaments. *J. Mol. Biol.* 99:445–459.

Matsudaira, P., and D. R. Burgess. 1982. Partial reconstruction of the microvillus core bundle: characterization of villin as a Ca^{++}-dependent, actin-bundling/depolymerizing protein. *J. Cell Biol.* 92: 648–656.

Matsudaira, P., E. Mandelkow, W. Renner, L. K. Hesterberg, and K. Weber. 1983. Role of fimbrin and villin in determining the interfilament distances of actin bundles. *Nature (Lond.).* 301:209–214.

O'Brien, E. J., J. M. Gillis, and J. Couch. 1975. Symmetry and molecular arrangement in paracrystals of reconstituted muscle thin filaments. *J. Mol. Biol.* 99:461–475.

Spudich, J. A., and S. Watt. 1971. The regulation of rabbit skeletal muscle contraction. *J. Biol. Chem.* 246:4866–4871.